April 2017

Thyroid ultrasound: state of the art. part 2 - focal thyroid lesions.

Manjiri Dighe
University of Washington, Seattle, USA

Richard Barr
Ohio Medical University, Rootstown, Ohio, USA

Jörg Bojunga
Goethe University Hospital, Frankfurt am Main, Germany.

Vito Cantisani
Policlinico Umberto I, University Sapienza, Rome, Italy.

Maria Cristina Chammas
Hospital das Clínicas, School of Medicine, Brazil

See next page for additional authors

Authors
Manjiri Dighe; Richard Barr; Jörg Bojunga; Vito Cantisani; Maria Cristina Chammas; David Cosgrove,; Xin Wu Cui; Yi Dong; Franziska Fenner; Maija Radzina; Sudhir Vinayak; Jun Mei Xu; and Christoph F Dietrich

Review

Med Ultrason 2017, Vol. 19, no. 2, 195-210
DOI: 10.11152/mu-999

Thyroid Ultrasound: State of the Art. Part 2 – Focal Thyroid Lesions

Manjiri Dighe[1], Richard Barr[2], Jörg Bojunga[3], Vito Cantisani[4], Maria Cristina Chammas[5], David Cosgrove6, Xin-Wu Cui[7], Yi Dong[8], Franziska Fenner[9], Maija Radzina[10], Sudhir Vinayak[11], Jun-Mei Xu[12], Christoph F Dietrich[13,14]

[1]Department of Radiology, University of Washington, Seattle, USA, [2]Department of Radiology, Northeastern Ohio Medical University, Rootstown, Ohio, USA and Southwoods Imaging, Youngstown, Ohio, USA, [3]Department of Internal Medicine 1, Endocrinology and Diabetology, Goethe University Hospital, Frankfurt am Main, Germany, [4]Department of Radiological Sciences, Oncology and Pathology, Policlinico Umberto I, University Sapienza, Rome, Italy, [5]Ultrasound Division, Department of Radiology, Hospital das Clínicas, School of Medicine, University of São Paulo, São Paulo, Brazil, [6]Division of Radiology, Imperial and Kings Colleges, London, UK, [7]Department of Internal Medicine 2, Caritas-Krankenhaus Bad Mergentheim, Germany, [8]Department of Ultrasound, Zhongshan Hospital, Fudan University, Shanghai, China, [9]Department of Surgery, Caritas-Krankenhaus Bad Mergentheim, Germany, [10]Diagnostic Radiology Institute, Paula Stradins Clinical University Hospital, Riga, Latvia, [11]Department of Imaging and Diagnostic Radiology, Aga Khan University Hospital, Nairobi, Kenya, [12]Department of Medical Ultrasound, Shanghai Tenth People's Hospital, Ultrasound Research and Education Institute, Tongji University School of Medicine, China, [13]Department of Internal Medicine 2, Caritas Hospital, Bad Mergentheim, Germany, [14]Sino-German Research Center of Ultrasound in Medicine, The First Affiliated Hospital of Zhengzhou University, Zhengzhou, China

Abstract

Accurate differentiation of focal thyroid nodules (FTL) and thyroid abnormalities is pivotal for proper diagnostic and therapeutic work-up. In these two part articles, the role of ultrasound techniques in the characterization of FTL and evaluation of diffuse thyroid diseases is described to expand on the recently published World Federation in Ultrasound and Medicine (WFUMB) thyroid elastography guidelines and review how this guideline fits into a complete thyroid ultrasound exam.

Keywords: thyroid; ultrasonography; elastography; color Doppler; contrast enhanced ultrasound (CEUS); point of care (POC).

Introduction

Focal thyroid lesions are common, with almost 50% of the population having thyroid nodules as per the autopsy database. The number of thyroid nodules also increases with age. Differentiation between benign and malignant nodules is important and even though fine needle aspiration (FNA) is the gold standard for diagnosis, pre-screening with ultrasound (US) is essential since performing FNA in all nodules is not feasible. US elastography is an additional non-invasive tool that is available and able to differentiate between benign and malignant nodules. This second part of the State of the Art Thyroid Ultrasound imaging deals with focal thyroid lesions and provides information about US and new techniques like elastography and contrast enhanced US (CEUS).

Received 20.11.2016 Accepted 22.12.2016
Med Ultrason
2017, Vol. 19, No 2, 195-210
Corresponding author: Prof. Dr. med. Christoph F. Dietrich
Department of Internal Medicine 2,
Caritas Krankenhaus, Uhlandstr. 7,
D-97980 Bad Mergentheim, Germany
Phone: 49 (0)7931 – 58 – 2201 / 2200
Fax: 49 (0)7931 – 58 – 2290
Email: Christoph.dietrich@ckbm.de

Benign thyroid nodules

In B-mode ultrasound, benign nodules generally present as isoechoic or hyperechoic, with well-defined margins, often with a hypoechoic halo, and with a variable vascularity at Doppler evaluation [1,2].

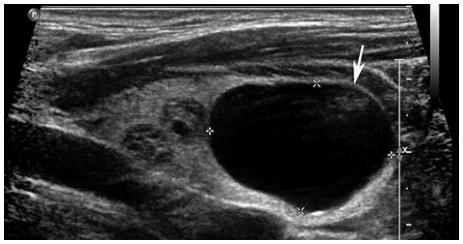

Fig 1. Cyst. A 29 year old female with multiple known thyroid nodules and difficulty swallowing due to a mass like feeling in the neck. A large anechoic cyst (arrow) was seen in the left lobe. No calcifications or ring down artifact were seen in this cyst.

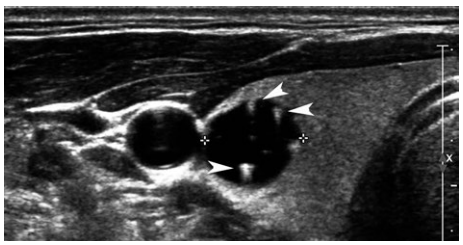

Fig 2. Colloid cyst. A 53 year old male with an incidental mass in the right lobe seen on CT. Transverse US shows a cystic mass in the right lobe with ring down artifact (arrowheads) seen in it consistent with a colloid cyst.

Cysts and Pseudocysts

The majority (67.3%) of incidentally detected thyroid lesions in children are cysts. True cysts occur as a result of dilatation of the ducts or tubules lined by epithelium and pseudocysts lack epithelial lining. True epithelial-lined thyroid cysts are rare. Most cystic thyroid lesions are pseudocysts from hyperplastic nodules that have undergone extensive degeneration, necrosis and hemorrhage into the parenchyma with fluid accumulation (fig 1) [3]. Colloid cysts may contain bright echogenic foci with comet-tail artifacts caused by the presence of microcrystals (fig 2) [4-6].

Calcification

Macrocalcifications are encountered in up to 20% of these lesions. To avoid false results at elastography, a macrocalcification must be excluded from the region of interest (ROI), as its stiffness alters the nodules stiffness assessment [7].

In addition to suspicious malignant nodules, a diffusely enlarged thyroid with numerous microcalcifications on US is defined as a thyroid malignancy and should be evaluated using FNA [8].

Multinodular goiter (MNG) (struma diffusa et nodosa)

Nodular goiters are clinically recognizable enlargements of the thyroid gland characterized by excessive growth and structural and/or functional transformation of one or several areas within the normal thyroid tissue. In the absence of thyroid dysfunction, autoimmune thyroid disease, thyroiditis, and thyroid malignancy, they constitute an entity described as simple nodular goiter [9].

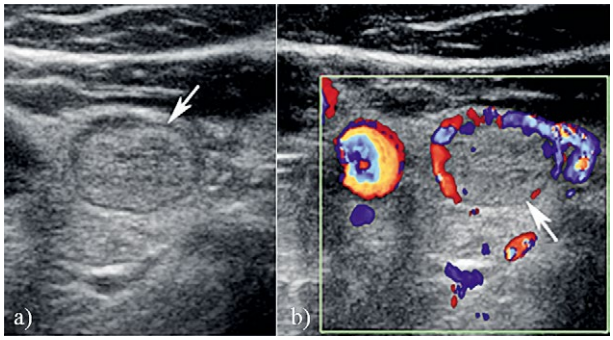

Fig 3. Benign isoechoic nodule in a 49 year old female with multiple thyroid nodules: a) B-mode and b) color Doppler US shows an isoechoic nodule (arrow) in the right lobe with regular margins, hypoechoic halo, well-defined margins and no calcifications (benign nodule at biopsy).

Conventional B-mode ultrasond

The benign thyroid nodule generally exhibits an isoecho or hyper-echo, well-defined margin and, often, a hypo-echoic halo (fig 3) [10].

Color Doppler imaging

Color Doppler imaging (CDI) may be able to differentiate between an "autoimmune" form of toxic multinodular goiter from an non-autoimmune form due to multiple autonomous nodules. Boi et al found in their study that increased vascularization on CDI was consistently found in autonomous 'hot' thyroid nodules on scintigraphy [11].

Elastography

The value of thyroid elastography for predicting malignancy in patients with nodular goiters was investigated by several authors. Different elastographic techniques were used by these authors and they found that all methods has both good sensitivity and specificity for predicting malignancy in thyroid nodules (fig 4) [12-16]. Also, inter- and intra-operator reproducibility of 'quasi-static' elastography is considered acceptable [17,18]. Thyroid nodules with VTQ values <2.16 m/s were all benign, which accounted for 60.2% of all benign nodules [19].

Contrast enhanced ultrasound

To date, no specific papers, to the best of our knowledge have been published focusing on CEUS in multinodular goiter.

Tips and tricks

Hot thyroid nodules are rarely malignant and therefore fine needle aspiration biopsy (FNAB) is not rec-

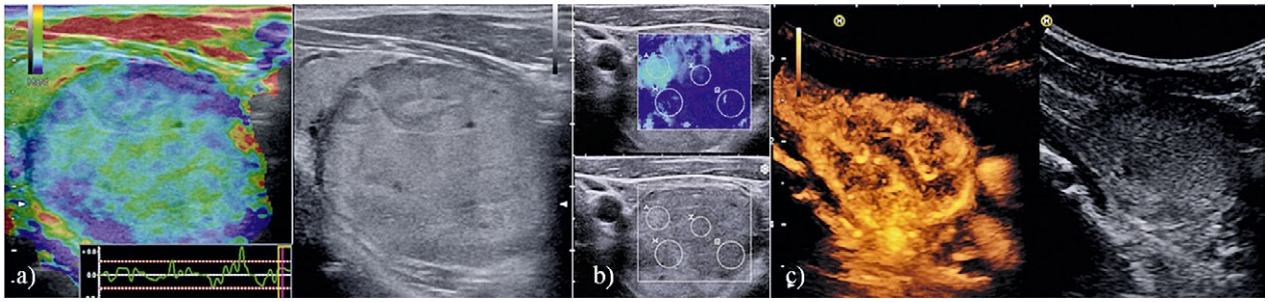

Fig 4. Multinodular goiter in a 55 year old male. The nodule is displayed using different elastographic techniques (a-b) and contrast enhanced ultrasound: a) shows the architecture using quasi static strain elastography technique and b) displays the measurement values using shear wave elastography. Primarily a neoplastic lesion was suspected and surgery performed. Comparative data between different manufacturerers are not published so far. Contrast enhanced ultrasound revealed inhomogenous enhancement due to regressive changes (c).

ommended. Nevertheless, the presence of concomitant indifferent or cold nodules on thyroid scintigraphy (especially if they are clinically suspicious) should prompt further evaluation.

Hyperplastic adenomatous nodules, adenoma

Autonomous thyroid adenomas occur unifocally, multifocally, or even in a disseminated fashion. Iodine deficiency and genetic disposition are etiological factors. Focal thyroid adenomas grow very slowly, often over the course of many years. As a rule, clinical symptoms of hyperthyroidism must be expected only if the nodule has reached a critical diameter of about 2.5 cm, although symptoms might occasionally occur with smaller volumes [20].

Conventional B-mode ultrasound

The majority of the hyperplastic adenomatous nodules are hypoechoic and clearly delineated nodules (fig 5). The nodules might show cystic degeneration and, in this case, can only be recognized as adenomas because of the hypoechoic edge with minimal residual tissue [20].

Color Doppler imaging

Demonstration of increased peripheral and central blood flow is an important indicator of functional activity, but only signifies autonomy to a certain extent in patients with hyperthyroidism. If a solitary adenoma is seen in the case of a hyperthyroid functional state, the probability that this represents carcinoma is extremely low. Regressive thyroid nodules, however, usually only show peripheral and not central vascularization [21].

Vascularization of a nodule must always be assessed in relationship to the surrounding 'normal' thyroid tissue. In accordance with rising hormone levels, perfusion of the autonomous nodules increases. Perfusion does not show a strict correlation with function, however, but is also dependent on the volume and grade of regressive change. The grade of perfusion (blood flow detected per unit of volume) of large nodules is smaller for equal func-

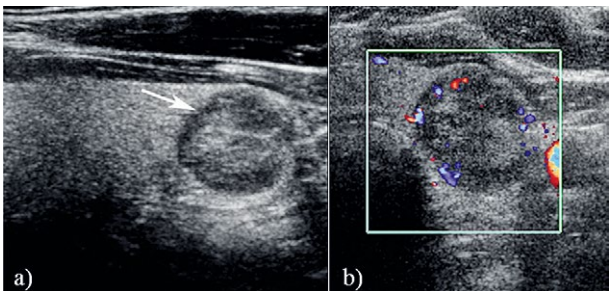

Fig 5. Adenoma. A 53 year old female presented for follow up US for thyroid nodule. Sagittal US (a) through the right lobe showed a hypoechoic nodule with no internal calcifications and with minimal internal vascularity on transverse color Doppler image (b).

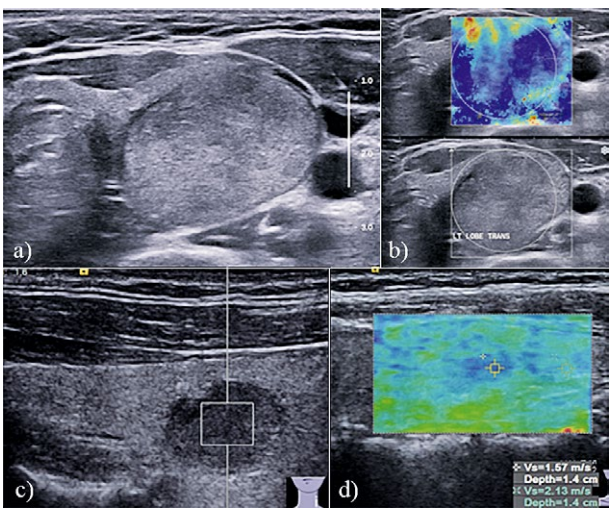

Fig 6. Benign adenoma – 2 cases. Case 1 – 45 year old male with an isoechoic nodule (a) in the left lobe with a halo around it. 2D SWE performed showed a predominantly soft lesion (b) with a stiffness value of 21.5kPa. FNA showed a benign adenoma. Case 2 (image c and d) – 56 year old with a hypoechoic nodule in the left lobe. ARFI measurement of nodule is 2.10 m/s (c). Shear wave velocity measurement by ROI (small boxes) in the color elastogram is 2.13m/s in the nodule and 1.57m/s in the adjacent thyroid gland (d).

tional states, especially in cases of regressive alteration. If these areas are destroyed by radioiodine treatment or instillation of alcohol or if hormone release is reduced by thyreostatic therapy, perfusion rate decreases again [20].

Elastography

Multiple studies involving elastography in thyroid nodules have found that adenomas are usually softer than other lesions (fig 6). A small number of adenomas can be harder if they have had prior hemorrhage, calcification or fibrosis. Samir et al in their study involving follicular lesions, found that at a cutoff value with 2D-SWE (shear wave elastography) of 22.30 kPa, SWE had a sensitivity of 82% and a specificity of 88% with a positive predictive value of 75% and a negative predictive value of 91% [22].

Contrast enhanced ultrasound

CEUS has been used to differentiate between benign and malignant nodules. Some authors reported that hypoenhancement is the most accurate US feature of malignancy on CEUS with high sensitivity, specificity and accuracy 82%, 85%, and 84%, respectively [23-27]. Three recent meta-analyses reported high-pooled accuracy of CEUS in diagnosing benign from malignant nodules with sensitivity, specificity, and positive and negative LR ranging 0.85-0.88, 0.87-0.90, 5.8-8.6 and 0.15-19 respectively [27-29].

Tips and tricks

In cases of doubt, biopsy or surgery must be performed. Scintigraphy might also be helpful, since cancer inside this lesion may be ruled out if there is an overactive (hot) nodule [30].

Malignant thyroid nodules

Ultrasound is essential in identifying suspicious nodules for cancer in the context of the high prevalence of benign lesions. Suspicious US features are: microcalcifications, marked hypoechogenicity, irregular margins with an absent halo, taller than wider shape, and intranodular vascularity greater than peripheral vascularity [31]. Sebag et al investigated the efficiency of SWE in predicting malignancy in solitary or multiple thyroid nodules. Using a cut-off level of 65 kPa, they could predict malignancy with sensitivity of 85.2%, specificity of 93.9% and positive predictive value (PPV) of 92.3% [32].

Compared with B mode US features for predicting malignancy, SWV ≥3.54 m/s has a higher sensitivity (79.27%), specificity (71.52%), PPV (26.75%) and negative predictive value (NPV) (96.34%). Thyroid nodule stiffness measured by virtual touch tissue imaging quantification (VTIQ) generated SWE is an independent predictor of thyroid cancer [33]. Grazhdani et al showed that ARFI imaging is a reproducible method with good diagnostic performance in differentiating benign and malignant nodules using the cut-off value of 2.455 m/s [34].

Studies with semi-quantitative Strain Elastography (SE) found that in benign nodules SR was 2.59±2.12 and in malignant ones 9.10±7.02 [28,35]. In another more recent study on 97 patients, the prediction of malignancy using strain ratio with cut-off value ≥2, sensitivity, specificity, PPV, and NPV of 97.3%, 91.7%, 87.8%, and 98.2% was obtained [7]. Strain index value greater than 4 on off-line processed elastograms was the strongest independent predictor of thyroid gland malignancy, with 96% specificity and 82% sensitivity. Two other elastographic criteria, which were evaluated on real time elastograms: a margin regularity score higher than 3 (88% specificity, 36% sensitivity) and a tumor area ratio higher than 1 (92% specificity, 46% sensitivity) also were associated with malignancy [12].

More recently, with the respect to the use of SR, two comprehensive meta-analysis were published. The first meta-analysis, in which qualitative and Strain-ratio results were provided, is the one published by Razavi et al [36]. In their paper, twenty-four studies provided relevant information on more than 2624 patients and 3531 thyroid nodules (927 malignant and 2604 benign). Six ultrasound features (echogenicity, calcifications, margins, halo sign, shape, and color Doppler flow pattern) were compared with elasticity score and strain ratio. The respective sensitivities and specificities were as follows: elasticity score, 82% and 82%; strain ratio, 89% and 82%; hypoechogenicity, 78% and 55%; micro-calcifications, 50% and 80%; irregular margins, 66% and 81%; absent halo sign, 56% and 57%; nodule vertical development, 46% and 77%; and intranodular vascularization, 40% and 61%. They showed and confirmed that ultrasound elastography appears to be both more sensitive and specific than each of the ultrasound features in thyroid nodule differentiation.

The second meta-analysis, published by Sun et al [37], assessed the diagnostic power of elastography in differentiating benign and malignant thyroid nodules for elasticity score and strain ratio assessment. A total of 5481 nodules in 4468 patients for elasticity score studies and 1063 nodules in 983 patients for strain ratio studies published until January 2013 were analyzed. The overall mean sensitivity and specificity of ultrasound elastography for differentiation of thyroid nodules were 0.79 (95% confidence interval [CI], 0.77-0.81) and 0.77 (95% CI, 0.76-0.79) for elasticity score assessment and 0.85 (95% CI, 0.81-0.89) and 0.80 (95% CI, 0.77-0.83) for strain ratio assessment, respectively. The areas under the curve for the elasticity score and strain ratio were 0.8941 and 0.9285.

A meta-analysis of qualitative SE published by Trimboli et al achieved AUC of 0.77 and concluded that SE has suboptimal diagnostic accuracy to diagnose thyroid nodules previously classified as indeterminate [38]. They advised for further studies using other elastographic approaches and combined real-time tissue elastography (RTE) and B-mode ultrasonography. More recently, Cantisani et al reported that ultrasound elastography (USE) with strain ratio should be considered a useful additional tool to colour Doppler US, since it improves characterization of thyroid nodules with indeterminate cytology [39].

When dealing with quasistatic strain USE with elasticity contrast index (ECI), values above 3 were the most accurate values cut-off for predicting the malignant nature of the nodules [40], This technique showed excellent inter-observer agreement [18].

Papillary thyroid carcinoma (PTC)

Papillary carcinoma is the most common form (80%) of thyroid malignancies [41].

Conventional B-mode ultrasound

PTC is diagnosed by conventional US based on its characteristic calcification, irregular shape, and heterogeneous internal echogenicity (fig 7) [42].

Color Doppler imaging

CDI of thyroid tumors is not useful for diagnosing papillary cancer, but it was reported to be clinically useful for diagnosing follicular cancer [43]. However, the diagnostic value of CDI remains controversial, probably due to its qualitative nature, poor inter-observer agreement and dependence on the sensitivity of the US technology and device settings. The 2015 ATA guidelines do not consider vascularity as an independent risk factor of malignancy on US [44].

Elastography

Dighe et al found good accuracy of carotid artery SE in diagnosing micropapillary carcinomas in small nodules (< 1 cm in transverse), ECI with a cut-off of 3.6 had a sensitivity of 100% and a specificity of 60% [45,46]. Thyroid stiffness index (TSI) calculated with elastography using carotid arterial pulsation, as the compression source was effective in helping distinguish between papillary carcinomas and other lesions because papillary carcinomas were stiffer than other lesions. Multiple nodules in a patient can be evaluated with elastography to select probable papillary carcinoma [45]. A semi-quantitative SE contrast index was effective in distinguishing small papillary thyroid carcinomas [46,47] (fig 8).

Ultrasound thyroid elastography using carotid artery pulsation appears to have the potential for noninvasively differentiating papillary carcinoma from benign nodular goiter. The TSI or papillary carcinoma was higher comparing with benign nodular goiter, indicating

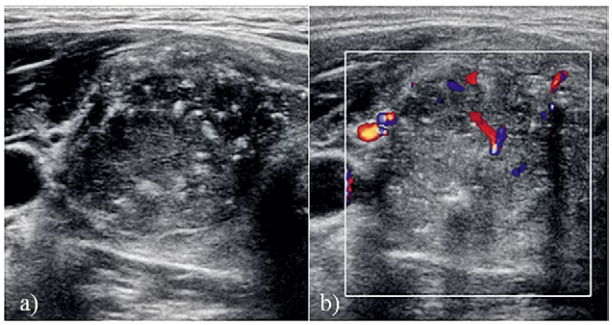

Fig 7. Papillary carcinoma in a 25 year old male presented with a palpable nodule in the right lobe. Transverse US image (a) showed a large hypoechoic nodule with multiple micro and macro calcifications and mild internal vascularity (b). FNA performed confirmed a papillary carcinoma.

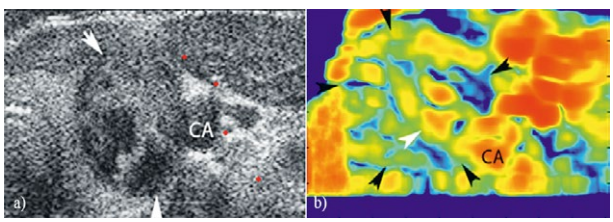

Fig 8. Carotid Pulsation based Elastography in a 40 year old female presented with an incidentally detected nodule in the left lobe. Transverse US (a) through the right lobe shows a mixed solid and cystic nodule in close proximity to the carotid artery. CA – carotid artery. Carotid artery based elastography (b) shows areas of increased stiffness within this nodule in the soft tissue portion of the nodule. This was shown to be a papillary carcinoma on FNA.

that papillary carcinoma is stiffer than a benign nodular goiter [48].

With regard to the thyroid nodules, the SWVs of papillary thyroid carcinoma were significantly higher than those of benign nodules. The AUROC curve was 0.83 and the SWV cut-off value was 2.36 m/s. The sensitivity, specificity, positive predictive value, negative predictive value and diagnostic accuracy were 70.0%, 84.3%, 28.6%, 96.1%. and 65.6%, respectively [49] (fig 9, fig 10). The most accurate SWE cut-off, 34.5 kPa for a 2 mm region of interest, achieved 76.9% sensitivity and 71.1% specificity for discriminating papillary cancer from benign nodules [50].

Contrast enhanced ultrasound

More recently Zhou et al reported that CEUS with quantitative evaluation was useful to predict papillary carcinomas. Compared with the peripheral parenchyma, 60 PTC nodules showed low heterogeneous enhancement and 2 nodules showed slightly high enhancement, and the peak intensity of CEUS in PTC was lower than in peripheral parenchyma [51].

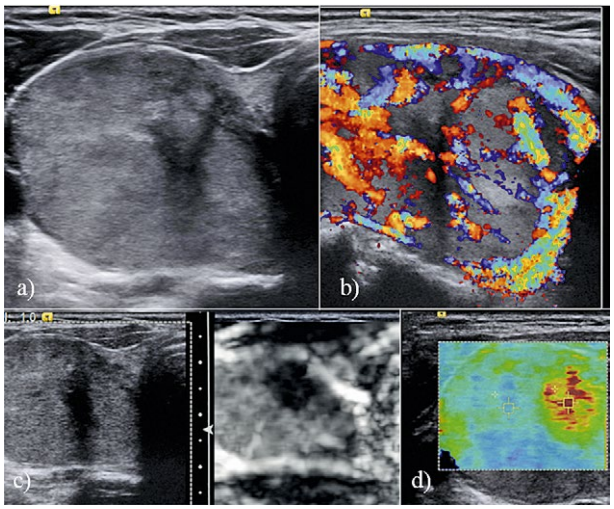

Fig 9. A 61 year old female with a 3.2 cm hypoechoic nodule seen in the right lobe on transverse image (a) that has markedly increased blood flow on color Doppler (b), a very stiff nodular component on strain elastography (c). On 2D-SWE (d) the nodule within the lesion had a stiffness value of 7.0m/s while the majority of the lesion has a stiffness of 2.28m/s. On biopsy the nodule was diagnosed to be a papillary carcinoma

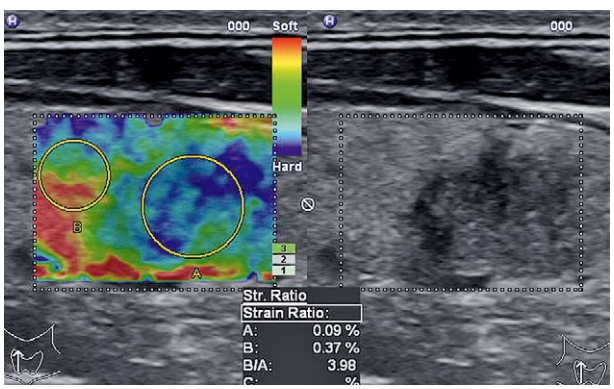

Fig 10. A 53 year old male patient with hypoechoic mass in the right thyroid lobe with irregular margins and heterogenous appearance. Strain elastography showed a relatively hard nodule with a strain ratio with the surrounding parenchyma of 3.98 and hence suspicious for malignancy. Histopathology after thyroidectomy showed a papillary thyroid carcinoma.

Tips and tricks

The cytological analysis based on Bethesda System (category IV) [52] is an independent predictor for malignancy in indeterminate thyroid nodules. Maia et al in their study showed that border irregularity and Bethesda System category IV were predictive factors of malignancy in indeterminate thyroid nodules, with an accuracy of 76.9%. This study confirmed a significant increase of risk for malignancy in thyroid nodules with indeterminate cytology showing Bethesda System category IV and suspicious features at US. These findings enhance our current limited predictive armamentarium and can be used to guide surgical decision making [53].

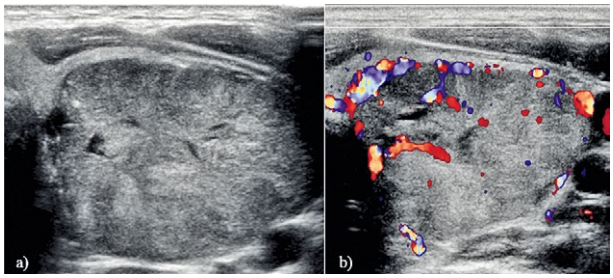

Fig 11. Follicular variant of papillary carcinoma in a 42 year old female with a palpable mass in the left lower lobe. Transverse US (a) of the left lobe showed a large hypoechoic mass with small cystic areas and some micro-calcifications and internal vascularity on color Doppler (b). Histopathology performed after resection showed the lesion to be a follicular variant of papillary carcinoma.

Follicular carcinoma

Follicular carcinoma accounts for approximately 5.1% of thyroid cancers and is more common in females than males [54,55]. The distinction between a benign and malignant follicular neoplasm can only be made by evaluating the presence of capsular or vascular invasion during a histological examination. The estimated rate of malignancy for follicular neoplasm is variable, ranging from 10-30 % [56].

Conventional B-mode ultrasound

The follicular variant of PTC, the second most common variant of thyroid carcinoma shows oval-to-round shapes more frequently compared with conventional PTCs, which usually have a typical taller-than-wide shape (fig 11). In addition, follicular PTCs may show isoechogenicity or hypoechogenicity rather than marked hypoechogenicity. A hypoechoic rim is more commonly seen in the follicular variant than in conventional PTC. Anuradha et al describes in a large retrospective study the usefulness off "nodule in nodule" sign and „hypoechoic internal septae" in differentiating follicular variant of PTC from benign thyroid nodules [57].

Color Doppler imaging

High-velocity pulsatile blood flow penetrating the tumor was found to be the characteristic finding of follicular carcinoma [43]. In thyroid follicular neoplasms, there were significant positive associations between predominantly central flow and malignancy and between predominantly peripheral flow and benign disease. However, power Doppler characteristics could not be used to rule out malignancy because 20% of malignant nodules had predominantly peripheral flow. For predicting malignancy a resistivity index cutoff of 0.75 showed good ac-

curacy, specificity, and negative predictive value but low sensitivity and positive predictive value (respectively, 91%, 97%, 92%, 40%, and 67%) [59].

Elastography

An important limitation of elastography is the lack of sensitivity for follicular thyroid carcinoma which showed an elastographic pattern similar to that found in benign nodules (fig 12) [60]. Follicular carcinomas can be soft and difficult to be differentiated from benign nodules, although some good results have also been reported both with SR SE [61] and with SWE [22]. In the latter paper a cut-off value of 22.30 kPa can help differentiate malignant from benign follicular thyroid lesions with sensitivity of 82%, specificity of 88%, and positive and negative predictive values of 75% and 91%, respectively.

Contrast enhanced ultrasound

In the study of Zhang et al the authors stated that heterogeneous enhancement correlated highly with a malignant diagnosis (sensitivity 88.2%, specificity, 92.5% positive predictive value, 91.8%, negative predictive value 89.1%, and accuracy 90.4%). In both mixed and solid nodules, ring enhancement is highly predictive of a benign finding [62].

Clinical decision making (biopsy, scintigraphy, etc)

Follicular carcinoma (fig 13) is less common and differentiating follicular carcinoma from adenomas is not possible with imaging. Because there are no specific imaging features the fine needle aspiration is required in these cases.

Anaplastic carcinoma

Anaplastic carcinoma is a highly aggressive form of thyroid cancer and accounts for 1-2% of primary thyroid malignancies. It typically occurs in elderly women with a peak incidence at 6th to 7th decades of life. A large number of these patients have a history of concurrent multinodular goiter [63,64].

Conventional B-mode ultrasound

Ultrasound features of anaplastic carcinoma include hypoechoic tumor, diffusely involving the entire lobe or gland, ill-defined margins, areas of necrosis, nodal or distant metastases, and extracapsular spread and vascular invasion (fig 14) [65]. In elderly women with common malignant features on ultrasound, the thyroid nodules with a maximum diameter greater than 5 cm, anteroposterior-to-transverse diameter ratio less than 1, and microcalcifications are highly likely to be anaplastic thyroid carcinoma [66]. Punctate calcifications are more commonly seen in anaplastic carcinoma compared to papillary carcinomas [66] but Suh et al found no difference in imaging features between anaplastic carcinoma and other types of aggressive thyroid carcinomas [67].

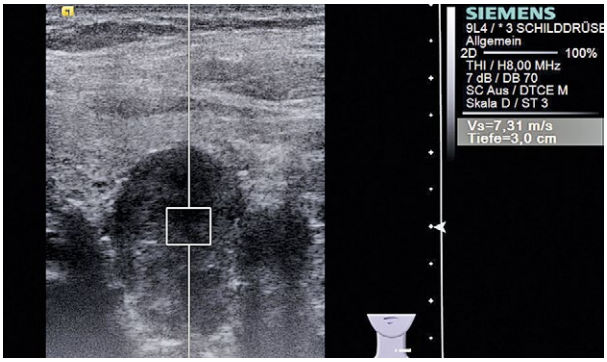

Fig 12. Ultrasound elastography in follicular variant of papillary carcinoma. A 63 year old male patient with markedly hypoechoic mass in the left thyroid lobe with a taller than wide shape and slightly irregular margins. Share wave elastography showed a very hard nodule with stiffness measurement of 7.3m/s. Histopathology after thyroidectomy showed a papillary thyroid carcinoma.

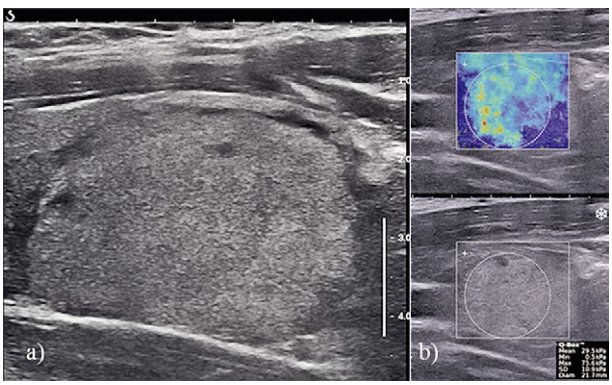

Fig 13. A 38 year old female patient with a isoechoic nodule in the left thyroid lobe with a halo and regular margins (a). SWE imaging showed a predominantly soft nodule (blue green on SWE color map (b)) with a few stiff areas in it (red – yellow on SWE color map), a mean stiffness of 29.5kPa and maximum stiffness of 75.6 kPa. FNA showed an indeterminate follicular nodule and histopathology after resection showed a follicular carcinoma.

Color Doppler imaging

Multiple small intranodular vessels are seen on color Doppler imaging [65].

Elastography

To date, no specific papers, to the best of our knowledge have been published focusing on anaplastic carcinoma. From personal experience in a series of 6 anaplastic carcinomas, the tumors are uniquely very hard on SE.

Contrast enhanced ultrasound

To date, no specific papers, to the best of our knowledge have been published focusing on anaplastic carcinoma

Tips and tricks

Patients with anaplastic carcinoma usually present later and have extensive involvement of surrounding

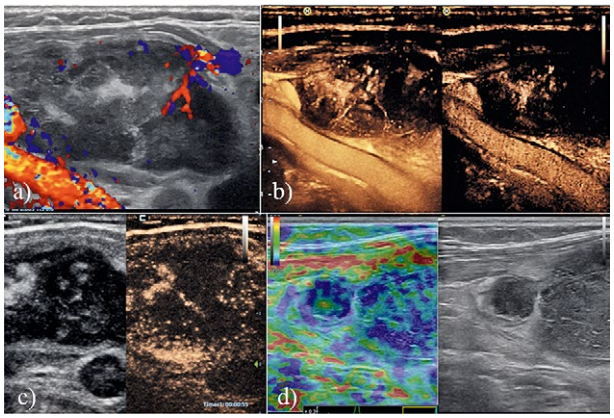

Fig 14. A 53 year old female with growing thyroid nodule. Anaplastic carcinoma was revealed by core needle biopsy. Color Doppler revealed only few vessels (a). Hypovascularity was proven by two contrast techniques, conventional (b) and using so-called microbubble tracing imaging (c). Elastography revealed stiff cervical lymph nodes (d).

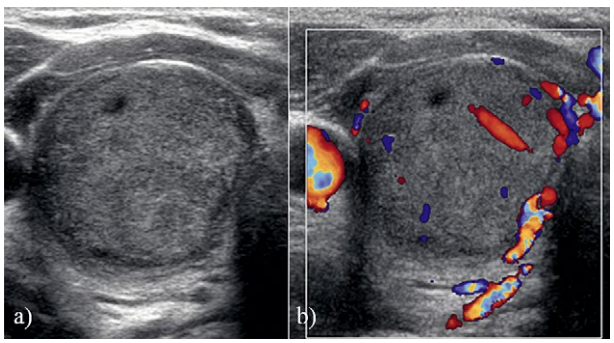

Fig 15. Medullary carcinoma in a 37 year old male with incidentally detected nodule on CT scan. Transverse US (a) of the right lobe showed a large hypoechoic predominantly solid nodule with mild internal vascularity on color Doppler (b). FNA showed cells suspicious for medullary carcinoma and this was confirmed on histopathology.

structures. Due to the fibrotic nature of this carcinoma, FNA may not be adequate and core biopsy may be required for diagnosis.

Medullary carcinoma

Medullary carcinoma (MTC) is thought to arise from parafollicular C-cells that secrete thyrocalcitonin. Only 5% of thyroid carcinomas are MTC, however 10-20% of patients with MTC have a family history of pheochromocytomas or hypercalcemia. MTC may be associated with MEN II-syndrome [68].

Conventional B-mode ultrasound

Ultrasound features of MTC include solid hypoechoic nodule with echogenic foci in 80-90% due to amyloid deposition or calcification (fig 15) [65]. Trimboli et al reported that MTC is frequently associated with features of aggressiveness, suggesting that careful preoperative US of MTC patients may better plan their surgical approach [69].

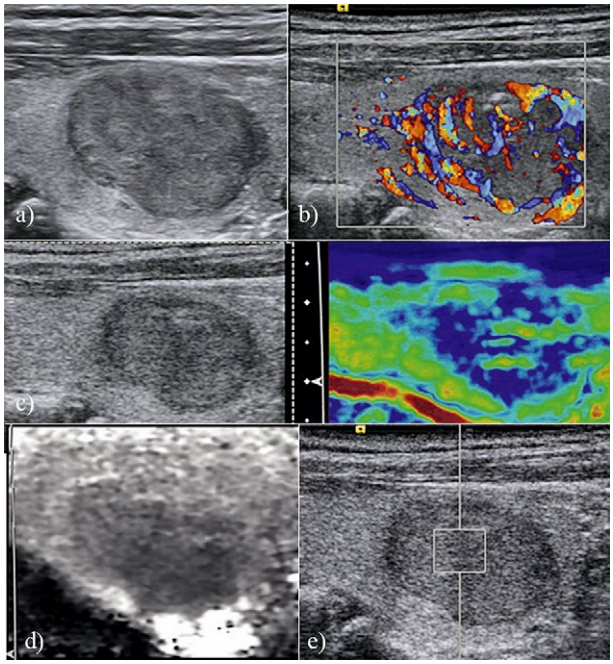

Fig 16. Ultrasound elastography in medullary thyroid carcinoma in a 72-year-old woman. A 20 mm thyroid nodule that appears as hypo-echogenicity, well defined margin, presence of halo sign, and rich intranodular and peripheral flow was found in left lobe of the thyroid at conventional US (a,b). The EI score 3 (c, the nodule is displayed predominantly in blue with few green areas/spots), VTI grade IV (d, most lesion is displayed in black with a small amount of white) and SWV of 2.71 m/s (e) on VTQ are assigned at elastography.

Color Doppler imaging

Chaotic intranodular vessels are seen in the tumor on color flow imaging [65].

Elastography

To date only few papers on MTC tumors have been reported. Andrioli et al recently reported their experience on 18 histologically proven MCTs, showing that at qualitative SE most of MTCs presented as soft elastographic pattern, more than half having a low-intermediate grade of elasticity. Therefore, qualitative elastography was reported to have no added value in these cases [70] (fig 16). Future technical developments to reduce the inter-observer and intra-observer variability are warranted. Most of the MTCs present an elastographic pattern of benignity suggesting that most of the MTC lesions are not hard. Indeed, the hardest medullary lesions (ES4) were those with other US features suggestive of malignancy in our series.

Contrast enhanced ultrasound

To date, no specific papers, to the best of our knowledge have been published focusing on MTC.

Tips and tricks

Calcifications are commonly seen in MCT.

Lymphoma

Primary thyroid lymphoma (PTL) is a rare malignant disease (1-3% of all thyroid malignancies), which can become life threatening because of airway obstruction due to rapidly growing mass. Patients usually have a history of prior Hashimoto's disease. Non-Hodgkin's lymphoma can more often involve the thyroid gland than Hodgkin's disease. Typical presentation is an elderly female with a rapidly increasing mass. Involvement may be focal or diffuse with commonly extrathyroidal spread and vascular invasion [71,72].

Conventional B-mode ultrasound

The sonographic patterns of PTL could be classified into diffuse and nodular or segmental types, based on the distribution of hypoechoic and echogenic structures within the lesions. Some common US characteristics suggesting thyroid malignancy could not facilitate differentiation of PTL from nodular goiter. However, a central blood flow pattern would favor the diagnosis of primary thyroid lymphoma, whereas a peripheral pattern would suggest the diagnosis of nodular goiter [73]. Other authors report that although some common features were found, the sonographic appearance of PTL is nonspecific, especially for the diffuse type [74]. Yang et al showed in 12 patients with PTL diffuse heterogeneous hypoechoic parenchyma with intervening echogenic septa-like structures in 3 patients (25.0%), markedly hypoechoic masses in 8 patients (66.7%), and a mixed pattern in one patient (8.3 %) (fig 17) [75].

Color Doppler imaging

A central blood flow pattern would highly suggest the diagnosis of PTL rather than nodular goiter [73].

Elastography

To date, no specific papers, to the best of our knowledge have been published focusing on thyroid lymphoma, though some author's speculate that elastography may be able to differentiate between nodules due to chronic autoimmune thyroiditis and lymphoma, however data regarding this is lacking [76].

Contrast enhanced ultrasound

To date, no specific papers, to the best of our knowledge have been published focusing on thyroid lymphoma

Tips and tricks

Prompt and accurate detection and diagnosis in the early phase of PTL are crucial for the treatment of this disease. However, due to lack of standardized diagnostic procedures and methods, PTL can be easily missed or misdiagnosed [75].

Sarcoma

Ultrasound evaluation of proved primary thyroid sarcomas (PTS) was reported for 36 patients in systematic review by Surov et al [77]. The following data were retrieved for the identified sarcomas: localization, size, homogeneity, internal texture, and margin characteristics. In most cases, PTS occurred in patients over 40 years of age, with a peak incidence for the group aged 60-79 years. Angiosarcoma was diagnosed in 29 cases (20.4%), followed by malignant hemangioendothelioma (n=23, 16.3%), malignant fibrous histiocytoma (n=20, 14.1%), leiomyosarcoma (n=16, 11.3%), and fibrosarcoma (n=13, 9.2%). In most patients (n=113, 79.6%), PTS manifested clinically as a painless goiter. On ultrasound, PTS were predominantly mixed hypo-to-hyperechoic in comparison to the normal thyroid tissue. In 26.8%, infiltration of the adjacent organs was seen. The trachea or esophagus was affected more frequently in patients with malignant histiocytoma and liposarcoma. The described features should be taken into consideration in the differential diagnosis of thyroid tumors.

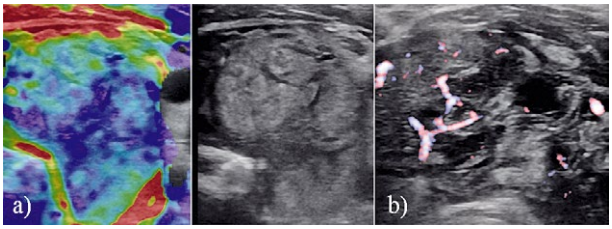

Fig 17. Diffuse large B cell lymphoma in a 53 year old female with a large rapidly growing mass in the left thyroid lobe with irregular margins and heterogeneous appearance and central blood flow pattern. Strain elastography showed a hard nodule. Core needle biopsy showed a diffuse large B cell lymphoma.

Metastasis

Conventional B-mode ultrasound

Metastatic carcinomas to the thyroid are rare in daily clinical practice. However, when encountered, they represent a diagnostic challenge, since it is difficult to distinguish them from primary thyroid lesions, especially when occurring in patients with occult malignant history [78]. There are no specific clinical features and few characteristic findings of metastatic thyroid carcinoma on imaging studies such as US and computed tomography (CT) [79]. The use of preoperative FNAB, with low morbidity and reasonable cost, has been emphasized as an effective and useful procedure for the diagnosis of metastatic thyroid cancer. Contrary to the wide consensus that FNAB is an accurate diagnostic tool, Chung et al reviewing the literature of metastasis reported a high false negative rate of 28.7%. Thus, one should remain suspicious for metastatic disease to the thyroid gland when FNAB is negative or indeterminate for malignant cells [80].

Color Doppler imaging

No specific information has been published about color Doppler imaging of metastases.

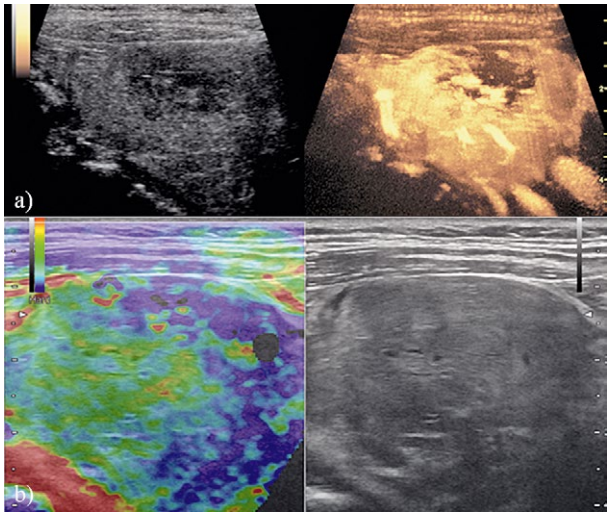

Fig 18. A 62 year old male patient with metachronic re-recurrence of thyroid metastases shown by contrast enhanced ultrasound with typical non enhancing areas (a) and heterogenous elastographic characteristics (b) corresponding to the typical finding of renal cell carcinoma.

Elastography

Metastatic carcinoma might also present as soft and might not be diagnosed with elastography (fig 18) [81].

Contrast enhanced ultrasound

To date, no specific papers, to the best of our knowledge have been published focusing on thyroid metastases.

Tips and tricks

Metastatic carcinoma has nonspecific imaging features and should be suspected if there is a history of malignancy in the patient. FNA might have to be modified to include core biopsy in case of suspicion of metastasis. The contrast behavior may mimic the typical enhancement pattern of the original tumor [44,54,82].

Differential diagnosis of focal thyroid disease

Rago et al evaluated tissue stiffness by elastography in a large group of patients with thyroid nodules who underwent surgery for compressive symptoms or suspicion of malignancy at FNA. Elastography displayed a sensitivity of 97%, a specificity of 100%, a positive predictive value of 100 % and a negative predictive value of 98%, independently from nodule size [83].

Monitoring after thyroidectomy

If indicated, percutaneous ethanol installation therapy (PEIT) may result in contraction of thyroid cysts or may be used for the treatment of autonomous lesions of the thyroid.

The value of scintigraphy

The clinical indications for thyroid scintigraphy, according to American Association of Clinical Endocrinologists medical guidelines for clinical practice for the diagnosis and management of thyroid nodules, are: 1- TSH level below the normal range, 2- Iodine-deficient areas even if the TSH level is in the low-normal range, 3- Suspected ectopic thyroid tissue or retrosternal goiter. Findings on thyroid scintigraphy are unspecific. A cold nodule may represent a benign lesion (like adenoma, cyst or hemorrhage) or a malignant one (well differentiated carcinoma, medullary or anaplastic carcinoma). Less than 20 % of cold nodules are actually malignant. A hot nodule is generally an autonomous or hypertrophic adenoma [84].

Although thyroid scintigraphy remains a standard radiologic study, thyroid US can be a practical alternative in many cases and the primary imaging modality in some situations such as during pregnancy and lactation and for evaluation and management of amiodarone-induced thyrotoxicosis.

The value of biopsy

FNA remains the most useful method of obtaining cellular diagnosis of any thyroid abnormality before treatment. In most situations it is the single most cost-effective investigation of a thyroid nodule. US guidance of the FNAB is an excellent means of ensuring accurate sampling of the area of interest. It provides greater accuracy as it enables the needle to be guided into impalpable nodules as well is into the solid component of a complex nodule. It has been report increased accuracy of FNAB by repeated biopsies after 3 months [85].

Although it is an effective and safe tool, FNA cytology does not alone provide all of the necessary information for clinical decision-making regarding thyroid nodules. Expert cytologists using the definitions established at the Bethesda conference report that between 2 % and 20 % of punctures are not satisfactory or do not provide diagnostic information. Furthermore, a portion of the remaining punctures do not provide conclusive results regarding benignancy or malignancy [86].

Stiffness can vary inside the nodule, which may be related to different tissue types, such as follicular cells, colloid, fibrosis, and necrosis. Elastography could guide the thyroid FNA biopsy to improve the sensitivity and specificity of the FNA in thyroid cancer detection and reduce the number of cases having an insufficient number of tissue samples for diagnosis [48].

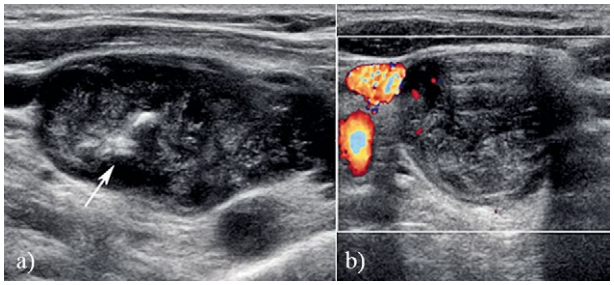

Fig 19. Abnormal lymph nodes – 45 year old male with known papillary carcinoma post resection presented for routine follow up. Oblique sagittal US (a) through the left neck showed a large hypoechoic nodule with internal calcifications (arrow) and abnormal internal vascularity (b). This was confirmed to be papillary carcinoma metastasis on FNA.

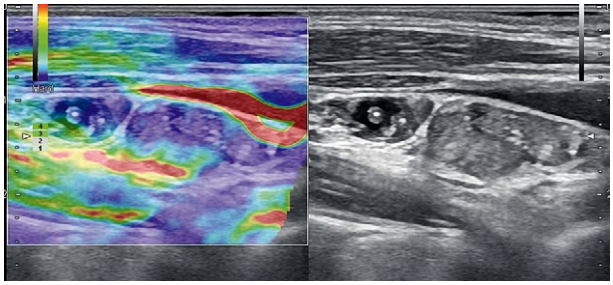

Fig 20. A 17 year old female with metastatic papillary carcinoma lymph nodes. Note the stiff lymph nodes.

Lymphadenopathy

US may demonstrate tumor spread by identifying enlarged lymph nodes (LN), vascular invasion, and local recurrence after surgery. US is frequently advocated as an useful imaging modality in LN evaluation with sensitivity and specificity close to other imaging techniques, and because it can also be used to guide biopsies (fig 19) [87]. Several US criteria have been reported: nodal size, shape, site, outline, internal appearance, and behavior after contrast administration. However, there is not unanimous consent about these criteria and the introduction of USE and CEUS have opened new possibilities. Lyshchik et al reported their study to assess the diagnostic accuracy of strain elastography by evaluating 141 LN [12]. Using a strain ratio cut-off value of >1.5, strain elastography showed sensitivity, specificity, and accuracy values of 85%, 98%, and 92%, respectively. The 4-point color-coded US-elastography scale is frequently used for detecting malignant LN. In general, metastatic LN demonstrate higher stiffness than benign LN. So, elastographic scale scores of 1-2 indicate benign LN, and elastographic scale scores of 3-4 indicate malignant LN [88].

Rubaltelli studied 53 patients, 28 of whom had malignant forms of lymphadenopathy (metastatic in 21 cases, non-Hodgkin lymphomas in 7) [89]. Compared with cytological and/or histological diagnosis, US-elastography achieved a sensitivity of 75%, specificity of 80%, and accuracy of 77% with positive and negative predictive values of 80% and 70%, respectively. More recently Ying et al reported results of a meta-analysis, based on 9 studies that showed analyzed 835 LN pooled sensitivity and specificity values for detecting malignancies 74% and 90% for elastographic scale and 88% and 81% using strain ratios, respectively [90]. According to those results, they concluded that SE could potentially help to select suspicious LN for biopsy. About SWE and ARFI there are relatively few clinical studies that have compared ARFI imaging and supersonic shear imaging. Bhatia et al have reported that the median elastic modulus of malignant LN is higher than that of benign lymph nodes [50]. However, discrimination was low because the optimal cut-off value of 30.2 kPa demonstrated sensitivity, specificity, and accuracy values of 41.9%, 100%, and 61.8%, respectively. Another study has reported that the maximum elastic modulus can be used to differentiate malignant LN, and that a cut-off value of 19.4 kPa resulted in accuracy, sensitivity, and specificity values of 94%, 91%, and 97%, respectively (fig 20) [91]. At CEUS, reactive nodes usually present with intense homogeneous enhancement, whereas perfusion defects are a sign of metastatic involvement [92,93]. Scant or absent perfusion can be observed in widespread metastatic infiltration, reflecting presence of large areas of necrosis. Based on these features, Rubaltelli et al found a specificity, sensitivity, and accuracy in differentiation between benign and metastatic nodes of 93%, 92%, and 93%, respectively [94]. Furthermore, when signal time-intensity curves are generated and parametric images are calculated the perfusion parameters, such as the arrival time, time to peak, and peak signal intensity, the difference between peak signal intensity in hyper enhancing and hypo enhancing regions are higher in metastatic LN [95].

However, cervical LN diagnosis relies on FNA, which crucially depends on the experience and ability of the cytopathologist, and may be a challenging diagnostic category as cervical LN could harbor metastasis from a multiplicity of extrathyroidal malignancies or be affected by several non-tumoral diseases [96,97].

Parathyroid

Four parathyroid glands are normally present, 2 on each side, one superior and one inferior. They are located posterior to the thyroid gland. Ectopic and supernumerary parathyroid glands can occur as well. Ectopic superior glands may be undescended, parapharyngeal

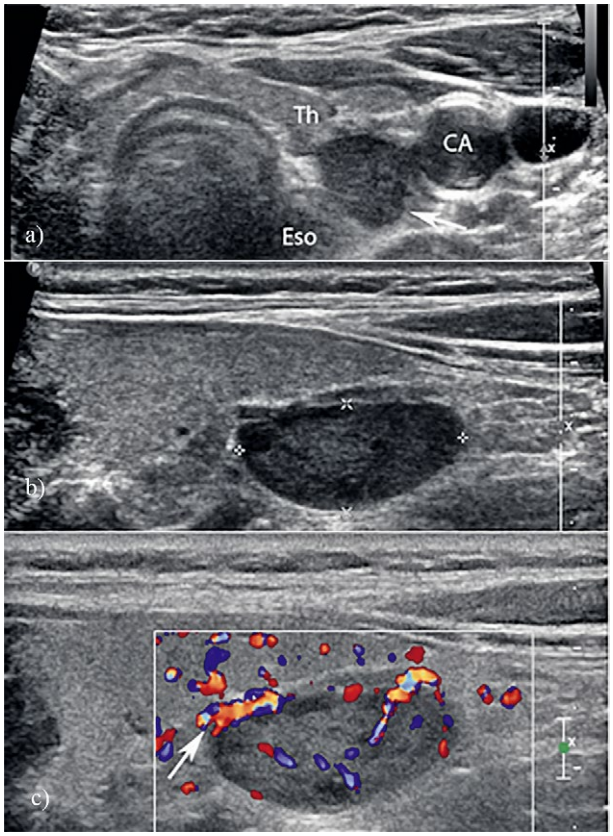

Fig 21. Parathyroid adenoma in a 44 year old female with elevated serum calcium levels. Transverse (a) and sagittal (b) US through the left lower neck showed a hypoechoic mass posterior to the thyroid gland (Th). CA – carotid artery, Eso – esophagus. Color Doppler US (c) showed significant internal vascularity and an enlarged inferior thyroid artery (arrow).

near the piriform sinus, retropharyngeal, or retrotracheal. Ectopic inferior glands are more variable and can be undescended near the carotid bulb, within the carotid sheath, inferolateral to the lower pole of the thyroid in the thyrothymic tract, intrathyroidal, or in the thymus or mediastinum [98]. The blood supply to the superior and inferior parathyroid glands comes from the inferior thyroidal artery in most patients and tracing an enlarged inferior thyroidal branch is often of help in locating a parathyroid adenoma [2].

Conventional B-mode ultrasound

Parathyroid adenomas are typically uniformly hypoechoic relative to the thyroid gland and appear as well-circumscribed oval nodules (fig 21). Large adenomas may assume a bilobed or lobulated configuration or develop internal cystic changes. When seen immediately adjacent to the thyroid, the curvilinear echogenic margin of the thyroid capsule should be appreciable and will help in localizing the nodule as external to the thyroid [6].

Color Doppler imaging

Parathyroid adenomas are highly vascular lesions supplied by a prominent extrathyroidal feeding artery, usually the inferior thyroid artery. The feeding artery enters the adenoma at one pole along its long axis. The vascularity of an adenoma is peripheral in nature, encircling 90 to 270 degrees of the gland, however the internal vascular flow is variable [2,82,98].

Elastography

Limited information is available about the utility of US elastography in parathyroid diseases. A single study by Ünlütürk et al involving 72 patients with 93 parathyroid lesions found elasticity scores of 3 and 4 in all the parathyroid adenomas. The median strain ratio of parathyroid lesions showed that parathyroid adenomas showed a significantly higher level of stiffness compared to hyperplasias [30].

Contrast enhanced ultrasound

Agha et al have shown a sensitivity of 97% in detection of correct quadrant of the pathological parathyroid gland and 99% for correct side in comparison with 70% for conventional US [99]. In a follow up study, Agha et al showed that CEUS had a sensitivity of 95.9% for the detection of pathological parathyroid glands in comparison to 60.8% for (99m) Technetium-sestamibi scintigraphy. Sensitivity of CEUS in patients with negative scintigraphy was 96.3% [100,101].

Tips and tricks

Exophytic thyroid nodules can be mistaken for parathyroid lesions and rarely some parathyroid adenomas are located within the thyroid gland. If there is a suspicion for an intrathyroid parathyroid adenoma, samples from the FNA should also be sent for measurement of tissue parathyroid hormone levels; which will be diagnostic for parathyroid adenoma [102].

Conclusion

This chapter in the two part series describes the utility of ultrasound and new techniques in ultrasound like elastography and ultrasound contrast in evaluation of thyroid nodules, lymph nodal disease and parathyroid lesions [103-104].

Conflict of interest: none

References

1. Reiners C, Wegscheider K, Schicha H, et al. Prevalence of thyroid disorders in the working population of Germany: ultrasonography screening in 96,278 unselected employees. Thyroid 2004;14:926-932.

2. Kim C, Baek JH, Ha E, et al. Ultrasonography features of medullary thyroid cancer as predictors of its biological behavior. Acta Radiol 2016. doi:10.1177/0284185116656491.
3. Kini SR. Cysts and cystic lesion of the thyroid. In: Thyroid cytopathology: an atlas and text: Lipincott Williams & Wilkins, 2008:369-384.
4. Avula S, Daneman A, Navarro OM, Moineddin R, Urbach S, Daneman D. Incidental thyroid abnormalities identified on neck US for non-thyroid disorders. Pediatr Radiol 2010;40:1774-1780.
5. Chang YW, Hong HS, Choi DL. Sonography of the pediatric thyroid: a pictorial essay. J Clin Ultrasound 2009;37:149-157.
6. Rho MH, Kim DW. Long-Term Ultrasonography Follow-Up of Thyroid Colloid Cysts at the Health Center: A Single-Center Study. Int J Endocrinol 2015;2015:324581.
7. Cantisani V, D'Andrea V, Biancari F, et al. Prospective evaluation of multiparametric ultrasound and quantitative elastosonography in the differential diagnosis of benign and malignant thyroid nodules: preliminary experience. Eur J Radiol 2012;81:2678-2683.
8. Lee KY, Hong HS, Lee EH, et al. Imaging and clinical features of thyroid cancer in children and adolescents. J Korean Soc Radiol 2011;65:181-189.
9. Hegedus L, Bonnema SJ, Bennedbaek FN. Management of Simple Nodular Goiter: Current Status and Future Perspectives. Endocr Rev 2003;24:102-132.
10. Gharib H, Papini E, Paschke R, et al. American Association of Clinical Endocrinologists, Associazione Medici Endocrinologi, and EuropeanThyroid Association Medical Guidelines for Clinical Practice for the Diagnosis and Management of Thyroid Nodules. Endocr Pract 2010;16 Suppl 1:1-43.
11. Boi F, Loy M, Piga M, Serra A, Atzeni F, Mariotti S. The usefulness of conventional and echo colour Doppler sonography in the differential diagnosis of toxic multinodular goitres. Eur J Endocrinol 2000;143:339-346.
12. Lyshchik A, Higashi T, Asato R, et al. Thyroid gland tumor diagnosis at US elastography. Radiology 2005;237:202-211.
13. Rago T, Di Coscio G, Basolo F, et al. Combined clinical, thyroid ultrasound and cytological features help to predict thyroid malignancy in follicular and Hupsilonrthle cell thyroid lesions: results from a series of 505 consecutive patients. Clin Endocrinol (Oxf) 2007;66:13-20.
14. Kagoya R, Monobe H, Tojima H. Utility of elastography for differential diagnosis of benign and malignant thyroid nodules. Otolaryngol Head Neck Surg 2010;143:230-234.
15. Azizi G, Keller J, Lewis M, Puett D, Rivenbark K, Malchoff C. Performance of elastography for the evaluation of thyroid nodules: a prospective study. Thyroid 2013;23:734-740.
16. Bojunga J, Herrmann E, Meyer G, Weber S, Zeuzem S, Friedrich-Rust M. Real-time elastography for the differentiation of benign and malignant thyroid nodules: a meta-analysis. Thyroid 2010;20:1145-1150.
17. Monpeyssen H, Tramalloni J, Poirée S, Hélénon O, Correas JM. Elastography of the thyroid. Diagn Interv Imaging 2013;94:535-544.
18. Lim DJ, Luo S, Kim MH, Ko SH, Kim Y. Interobserver agreement and intraobserver reproducibility in thyroid ultrasound elastography. AJR Am J Roentgenol 2012;198:896-901.
19. Li T, Zhou P, Zhang X, Ding M, Yuchi M, Li Y. Diagnosis of thyroid nodules using virtual touch tissue quantification value and anteroposterior/transverse diameter ratio. Ultrasound Med Biol 2015;41:384-392.
20. Blank W, Braun B. Sonography of the Thyroid-Part 2: Thyroid Inflammation, Impairmant of Thyroid Function and Interventions. Ultraschall Med 2008;29:128-155.
21. Clark KJ, Cronan JJ, Scola FH. Color Doppler sonography: anatomic and physiologic assessment of the thyroid. J Clin Ultrasound 1995;23:215-223.
22. Samir AE, Dhyani M, Anvari A, et al. Shear-Wave Elastography for the Preoperative Risk Stratification of Follicular-patterned Lesions of the Thyroid: Diagnostic Accuracy and Optimal Measurement Plane. Radiology 2015;277:565-573.
23. Deng J, Zhou P, Tian SM, Zhang L, Li JL, Qian Y. Comparison of diagnostic efficacy of contrast-enhanced ultrasound, acoustic radiation force impulse imaging, and their combined use in differentiating focal solid thyroid nodules. PLoS One 2014;9:e90674.
24. Nemec U, Nemec SF, Novotny C, Weber M, Czerny C, Krestan CR. Quantitative evaluation of contrast-enhanced ultrasound after intravenous administration of a microbubble contrast agent for differentiation of benign and malignant thyroid nodules: assessment of diagnostic accuracy. Eur Radiol 2012;22:1357-1365.
25. Cantisani V, Consorti F, Guerrisi A, et al. Prospective comparative evaluation of quantitative-elastosonography (Q-elastography) and contrast-enhanced ultrasound for the evaluation of thyroid nodules: preliminary experience. Eur J Radiol 2013;82:1892-1898.
26. Wu Q, Wang Y, Li Y, Hu B, He ZY. Diagnostic value of contrast-enhanced ultrasound in solid thyroid nodules with and without enhancement. Endocrine 2016;53:480-488.
27. Ma X, Zhang B, Ling W, et al. Contrast-enhanced sonography for the identification of benign and malignant thyroid nodules: Systematic review and meta-analysis. J Clin Ultrasound 2016;44:199-209.
28. Sun B, Lang L, Zhu X, Jiang F, Hong Y, He L. Accuracy of contrast-enhanced ultrasound in the identification of thyroid nodules: a meta-analysis. Int J Clin Exp Med 2015;8:12882-12889.
29. Yu D, Han Y, Chen T. Contrast-enhanced ultrasound for differentiation of benign and malignant thyroid lesions: meta-analysis. Otolaryngol Head Neck Surg 2014;151:909-915.
30. Nabipour I, Kalantarhormozi M, Assadi M. Thyroid Nodule Characterization Using Combined Fine-Needle Aspiration and (99m)Tc-Sestamibi Scintigraphy Strategy. AJR Am J Roentgenol 2016;207:W21.
31. Cantisani V, Lodise P, Grazhdani H, et al. Ultrasound elastography in the evaluation of thyroid pathology. Current status. Eur J Radiol 2014;83:420-428.
32. Sebag F, Vaillant-Lombard J, Berbis J, et al. Shear wave elastography: a new ultrasound imaging mode for the dif-

ferential diagnosis of benign and malignant thyroid nodules. J Clin Endocrinol Metab 2010;95:5281-5288.
33. Azizi G, Keller JM, Mayo ML, et al. Thyroid nodules and shear wave elastography: a new tool in thyroid cancer detection. Ultrasound Med Biol 2015;41:2855-2865.
34. Grazhdani H, Cantisani V, Lodise P, et al. Prospective evaluation of acoustic radiation force impulse technology in the differentiation of thyroid nodules: accuracy and interobserver variability assessment. J Ultrasound 2014;17:13-20.
35. Ning CP, Jiang SQ, Zhang T, Sun LT, Liu YJ, Tian JW. The value of strain ratio in differential diagnosis of thyroid solid nodules. Eur J Radiol 2012;81:286-291.
36. Razavi SA, Hadduck TA, Sadigh G, Dwamena BA. Comparative effectiveness of elastographic and B-mode ultrasound criteria for diagnostic discrimination of thyroid nodules: a meta-analysis. AJR Am J Roentgenol 2013;200:1317-1326.
37. Sun J, Cai J, Wang X. Real-time ultrasound elastography for differentiation of benign and malignant thyroid nodules: a meta-analysis. J Ultrasound Med 2014;33:495-502.
38. Trimboli P, Guglielmi R, Monti S, et al. Ultrasound sensitivity for thyroid malignancy is increased by real-time elastography: a prospective multicenter study. J Clin Endocrinol Metab 2012;97:4524-4530.
39. Cantisani V, Maceroni P, D'Andrea V, et al. Strain ratio ultrasound elastography increases the accuracy of colour-Doppler ultrasound in the evaluation of Thy-3 nodules. A bi-centre university experience. Eur Radiol 2016;26:1441-1449.
40. Cantisani V, Lodise P, Di Rocco G, et al. Diagnostic accuracy and interobserver agreement of quasistatic ultrasound elastography in the diagnosis of thyroid nodules. Ultraschall Med 2015;36:162-167.
41. Kim SH, Roh JL, Gong G, et al. Differences in the Recurrence and Survival of Patients with Symptomatic and Asymptomatic Papillary Thyroid Carcinoma: An Observational Study of 11,265 Person-Years of Follow-up. Thyroid 2016;26:1472-1479.
42. Grant EG, Tessler FN, Hoang JK, et al. Thyroid Ultrasound Reporting Lexicon: White Paper of the ACR Thyroid Imaging, Reporting and Data System (TIRADS) Committee. J Am Coll Radiol 2015;12:1272-1279.
43. Fukunari N, Nagahama M, Sugino K, Mimura T, Ito K, Ito K. Clinical evaluation of color Doppler imaging for the differential diagnosis of thyroid follicular lesions. World J Surg 2004;28:1261–1265.
44. Ignee A, Straub B, Brix D, Schuessler G, Ott M, Dietrich CF. The value of contrast enhanced ultrasound (CEUS) in the characterisation of patients with renal masses. Clin Hemorheol Microcirc 2010;46:275-290.
45. Dighe M, Bae U, Richardson ML, Dubinsky TJ, Minoshima S, Kim Y. Differential diagnosis of thyroid nodules with US elastography using carotid artery pulsation. Radiology 2008;248:662-669.
46. Dighe M, Luo S, Cuevas C, Kim Y. Efficacy of thyroid ultrasound elastography in differential diagnosis of small thyroid nodules. Eur J Radiol 2013;82:e274-e280.
47. Cantisani V, Grazhdani H, Drakonaki E, et al. Strain US Elastography for the Characterization of Thyroid Nodules: Advantages and Limitation. Int J Endocrinol 2015;2015:908575.
48. Bae U, Dighe M, Dubinsky T, Minoshima S, Shamdasani V, Kim Y. Ultrasound thyroid elastography using carotid artery pulsation – Preliminary study. J Ultrasound Med 2007;26:797-805.
49. Fukuhara T, Matsuda E, Endo Y, et al. Correlation between quantitative shear wave elastography and pathologic structures of thyroid lesions. Ultrasound Med Biol 2015;41:2326-2332.
50. Bhatia KS, Tong CS, Cho CC, Yuen EH, Lee YY, Ahuja AT. Shear wave elastography of thyroid nodules in routine clinical practice: preliminary observations and utility for detecting malignancy. Eur Radiol 2012;22:2397-2406.
51. Zhou Q, Jiang J, Shang X, et al. Correlation of contrast-enhanced ultrasonographic features with microvessel density in papillary thyroid carcinomas. Asian Pac J Cancer Prev 2014;15:7449-7452.
52. Cibas ES, Ali SZ. The Bethesda System for Reporting Thyroid Cytopathology. Thyroid 2009;19:1159-1165.
53. Maia FF, Matos PS, Pavin EJ, Vassallo J, Zantut-Wittmann DE. Value of ultrasound and cytological classification system to predict the malignancy of thyroid nodules with indeterminate cytology. Endocr Pathol 2011;22:66-73.
54. Ignee A, Straub B, Schuessler G, Dietrich CF. Contrast enhanced ultrasound of renal masses. World J Radiol 2010;2:15-31.
55. Babcock DS. Thyroid disease in the pediatric patient: emphasizing imaging with sonography. Pediatr Radiol 2006;36:299-308.
56. Nikiforova MN, Lynch RA, Biddinger PW, et al. RAS point mutations and PAX8-PPAR gamma rearrangement in thyroid tumors: evidence for distinct molecular pathways in thyroid follicular carcinoma. J Clin Endocrinol Metab 2003;88:2318-2326.
57. Anuradha C, Manipadam M, Asha H, Dukhabandhu N, Abraham D, Paul M. Can New Ultrasound Signs Help in Identifying Follicular Variant of Papillary Carcinoma of Thyroid? – A Pilot Study. Ultrasound Int Open 2016;2:E47-E53.
58. Nikiforov YE, Seethala RR, Tallini G, et al. Nomenclature Revision for Encapsulated Follicular Variant of Papillary Thyroid Carcinoma: A Paradigm Shift to Reduce Overtreatment of Indolent Tumors. JAMA Oncol 2016;2:1023-1029.
59. De Nicola H, Szejnfeld J, Logullo AF, Wolosker AM, Souza LR, Chiferi V Jr. Flow pattern and vascular resistive index as predictors of malignancy risk in thyroid follicular neoplasms. J Ultrasound Med 2005;24:897–904.
60. Asteria C, Giovanardi A, Pizzocaro A, et al. US-elastography in the differential diagnosis of benign and malignant thyroid nodules. Thyroid 2008;18:523-531.
61. Cantisani V, Ulisse S, Guaitoli E, et al. Q-elastography in the presurgical diagnosis of thyroid nodules with indeterminate cytology. PLoS One 2012;7:e50725.
62. Zhang B, Jiang YX, Liu JB, et al. Utility of contrast-enhanced ultrasound for evaluation of thyroid nodules. Thyroid 2010;20:51-57.

63. Chiacchio S, Lorenzoni A, Boni G, Rubello D, Elisei R, Mariani G. Anaplastic thyroid cancer: prevalence, diagnosis and treatment. Minerva Endocrinol 2008;33:341-357.
64. Giuffrida D, Gharib H. Anaplastic thyroid carcinoma: current diagnosis and treatment. Ann Oncol 2000;11:1083-1089.
65. Wong KT, Ahuja AT. Ultrasound of thyroid cancer. Cancer Imaging 2005;5:157-166.
66. Xu X, Yang X, Zhao RN, et al. Comparison of ultrasonic features between anaplastic thyroid carcinoma and papillary thyroid carcinoma. Zhongguo Yi Xue Ke Xue Yuan Xue Bao 2015;37:71-74.
67. Suh HJ, Moon HJ, Kwak JY, Choi JS, Kim EK. Anaplastic thyroid cancer: ultrasonographic findings and the role of ultrasonography-guided fine needle aspiration biopsy. Yonsei Med J 2013;54:1400-1406.
68. Norton JA, Froome LC, Farrell RE, Wells SA Jr. Multiple endocrine neoplasia type IIb: the most aggressive form of medullary carcinoma. Surg Clin North Am 1979;59:109-118.
69. Trimboli P, Giovannella L, Valabrega S, et al. Ultrasound features of medullary thyroid carcinoma correlate with cancer aggressiveness: a retrospective multicenter study. J Exp Clin Cancer Res 2014;33:87.
70. Andrioli M, Trimboli P, Amendola S, et al. Elastographic presentation of medullary thyroid carcinoma. Endocrine 2014;45:153-155.
71. Anscombe AM, Wright DH. Primary malignant lymphoma of the thyroid – a tumour of mucosa associated lymphoid tissue: review of seventy-six cases. Histopathology 1985;9:81-87.
72. Burke JS, Butler JJ, Fuller LM. Malignant lymphomas of the thyroid. Cancer 1977;39:1587–1602.
73. Wang Z, Fu B, Xiao Y, Liao J, Xie P. Primary thyroid lymphoma has different sonographic and color Doppler features compared to nodular goiter. J Ultrasound Med 2015;34:317-323.
74. Xia Y, Wang L, Jiang Y, Dai Q, Li X, Li W. Sonographic appearance of primary thyroid lymphoma-preliminary experience. PLoS One 2014;9:e114080.
75. Yang L, Wang A, Zhang Y, Mu Y. 12 cases of primary thyroid lymphoma in China. J Endocrinol Invest 2015;38:739-744.
76. Menzilcioglu MS, Duymus M, Gungor G, et al. The value of real-time ultrasound elastography in chronic autoimmune thyroiditis. Br J Radiol 2014;87:20140604.
77. Surov A, Gottschling S, Wienke A, Meyer HJ, Spielmann RP, Dralle H. Primary Thyroid Sarcoma: A Systematic Review. Anticancer Res 2015;35:5185-5191.
78. Cantisani V, Lodise P, Di Cossimo C, et al. Metastatic signet ring cell carcinoma presenting as a thyroid diffuse involvement: report of a case studied with Q-elastographic and acoustic radiation force impulse imaging features. Tumori 2013;99:e84-e87.
79. Medas F, Calo PG, Lai ML, Tuveri M, Pisano G, Nicolosi A. Renal cell carcinoma metastasis to thyroid tumor: a case report and review of the literature. J Med Case Rep 2013;7:265.
80. Chung AY, Tran TB, Brumund KT, Weisman RA, Bouvet M. Metastases to the thyroid: a review of the literature from the last decade. Thyroid 2012;22:258-268.
81. Oliver C, Vaillant-Lombard J, Albarel F, et al. What is the contribution of elastography to thyroid nodules evaluation? Ann Endocrinol (Paris) 2011;72:120-124.
82. Barr RG, Peterson C, Hindi A. Evaluation of indeterminate renal masses with contrast-enhanced US: a diagnostic performance study. Radiology 2014;271:133-142.
83. Rago T, Scutari M, Santini F, et al. Real-time elastosonography: useful tool for refining the presurgical diagnosis in thyroid nodules with indeterminate or nondiagnostic cytology. J Clin Endocrinol Metab 2010;95:5274-5280.
84. Lee ES, Kim JH, Na DG, et al. Hyperfunction Thyroid Nodules: Their Risk for Becoming or Being Associated with Thyroid Cancers. Korean J Radiol 2013;14:643-652.
85. Mann CL, Cartwright L, Greenberg ML, Boyages S. Evaluating the usefulness of repeat fine needle biopsies of thyroid nodules in detecting tumours. A.C.P.M.R. Cytology (Newsletter) 1995;2.
86. Cibas ES, Ali SZ; NCI Thyroid FNA State of the Science Conference. The Bethesda system for reporting thyroid cytopathology. Am J Clin Pathol 2009;132:658-655.
87. Sohn YM, Hong IK, Han K. Role of [18F] fluorodeoxyglucose positron emission tomography-computed tomography, sonography, and sonographically guided fine-needle aspiration biopsy in the diagnosis of axillary lymph nodes in patients with breast cancer: comparison of diagnostic performance. J Ultrasound Med 2014;33:1013-1021.
88. Lo WC, Cheng PW, Wang CT, Liao LJ. Real-time ultrasound elastography: an assessment of enlarged cervical lymph nodes. Eur Radiol 2013;23:2351-2357.
89. Rubaltelli L, Corradin S, Dorigo A, et al. Differential diagnosis of benign and malignant thyroid nodules at elastosonography. Ultraschall Med 2009;30:175-179.
90. Ying L, Hou Y, Zheng HM, Lin X, Xie ZL, Hu YP. Real-time elastography for the differentiation of benign and malignant superficial lymph nodes: a meta-analysis. Eur J Radiol 2012;81:2576-2584.
91. Choi YJ, Lee JH, Lim HK, et al. Quantitative shear wave elastography in the evaluation of metastatic cervical lymph nodes. Ultrasound Med Biol 2013;39:935-940.
92. Stramare R, Scagliori E, Mannucci M, Beltrame V, Rubaltelli L. The role of contrast-enhanced gray-scale ultrasonography in the differential diagnosis of superficial lymph nodes. Ultrasound Q 2010;26:45-51.
93. Poanta L, Serban O, Pascu I, Pop S, Cosgarea M, Fodor D. The place of CEUS in distinguishing benign from malignant cervical lymph nodes: a prospective study. Med Ultrason 2014;16:7-14.
94. Rubaltelli L, Khadivi Y, Tregnaghi A, et al. Evaluation of lymph node perfusion using continuous mode harmonic ultrasonography with a second-generation contrast agent. J Ultrasound Med 2004;23:829-836.

95. Rubaltelli L, Corradin S, Dorigo A, et al. Automated quantitative evaluation of lymph node perfusion on contrast-enhanced sonography. AJR Am J Roentgenol 2007;188:977-983.
96. Kessler A, Rappaport Y, Blank A, Marmor S, Weiss J, Graif M. Cystic appearance of cervical lymph nodes is characteristic of metastatic papillary thyroid carcinoma. J Clin Ultrasound 2003;31:21-25.
97. Pacini F, Schlumberger M, Dralle H, et al; European Thyroid Cancer Taskforce. European consensus for the management of patients with differentiated thyroid carcinoma of the follicular epithelium. Eur J Endocrinol 2006;154:787-803.
98. Robbin ML, Lockhart ME, Barr RG. Renal imaging with ultrasound contrast: current status. Radiol Clin North Am 2003;41:963-978.
99. Agha A, Jung EM, Janke M, et al. Preoperative diagnosis of thyroid adenomas using high resolution contrast-enhanced ultrasound (CEUS). Clin Hemorheol Microcirc 2013;55:403-409.
100. Agha A, Hornung M, Schlitt HJ, Stroszczynski C, Jung EM. The role of contrast-enhancend ultrasonography (CEUS) in comparison with 99mTechnetium-sestamibi scintigraphy for localization diagnostic of primary hyperparathyroidism. Clin Hemorheol Microcirc 2014;58:515-520.
101. Prieditis P, Radzina M, Strumfa I, Narbuts Z, Ozolins A, Vanags A, Gardovskis A. Diagnostic value of contrast-enhanced ultrasound evaluation of malignant and benign solitary thyroid nodules. Proceedings of the Latvian Academy of Sciences Section B Natural Exact and Applied Sciences 70(1):1-6 · January 2016 DOI: 10.1515/prolas-2016-0001.
102. Dietrich CF, Bojunga J. Ultrasound of the thyroid. Z Gastroenterol 2015; 53:208-225.
103. Cosgrove D, Barr R, Bojunga J, Cantisani V, Chammas MC, Dighe M, Vinayak S, et al. WFUMB Guidelines and Recommendations on the Clinical Use of Ultrasound Elastography: Part 4. Thyroid. Ultrasound Med Biol 2017;43:4-26.
104. Dighe M, Barr R, BojungaJ, et al. Thyroid ultrasound: state of the art. Part 1 – thyroid ultrasound reporting and diffuse thyroid diseases. Med Ultrason 2017;1:79-93.